

# The dual timescales of gait adaptation: Initial stability adjustments followed by subsequent energetic cost adjustments

Sarah A. Brinkerhoff<sup>1,\*</sup>, Natalia Sánchez<sup>2,3</sup>, Meral N. Culver<sup>1</sup>, William M. Murrah<sup>4</sup>, Austin T. Robinson<sup>5</sup>, J. Danielle McCullough<sup>6</sup>, Matthew W. Miller<sup>1</sup>, Jaimie A. Roper<sup>1</sup>

<sup>1</sup>Department of Neurology, University of Alabama at Birmingham, Birmingham, AL, USA

<sup>2</sup>Department of Physical Therapy, Chapman University, Irvine, California, USA

<sup>3</sup>Fowler School of Engineering, Chapman University, Orange, California, USA

<sup>4</sup>Department of Educational Foundations, Leadership, and Technology, Auburn University, Auburn, Alabama, USA

<sup>5</sup>Department of Kinesiology, Indiana University Bloomington

<sup>6</sup>Edward Via College of Osteopathic Medicine, Auburn Campus, Auburn Alabama, USA

\*Corresponding Author:

Email: [sabrinkerhoff@uabmc.edu](mailto:sabrinkerhoff@uabmc.edu)

**Keywords:** gait mechanics, motor adaptation, energetic cost

## Summary statement

This study elucidates the complex dynamics of gait adaptation, highlighting rapid stability optimization and gradual adjustments in metabolic rate and step kinetics and kinematics, offering insights into energy-saving mechanisms.

## Abstract

Gait adaptation during bipedal walking allows people to adjust their walking patterns to maintain balance, avoid obstacles, and avoid injury. Adaptation involves complex processes that function to maintain stability and reduce energy expenditure. However, the processes that influence walking patterns during different points in the adaptation period remain to be investigated. We recruited seventeen young adults ages 19-35 to assess split-belt adaptation. We also assessed individual aerobic capacity to understand how aerobic capacity influences adaptation. We analyzed step lengths, step

length asymmetry (SLA), mediolateral margins of stability, positive, negative, and net mechanical work rates, as well as metabolic rate during adaptation. We used dual-rate exponential mixed-effects regressions to estimate the adaptation of each measure over two timescales. Our results indicate that mediolateral stability adapts over a single timescale in under 1 minute, while mechanical work rates, metabolic rate, step lengths, and step length asymmetry adapt over two distinct timescales, ranging from 3.5 to 11.2 minutes. We then regressed mediolateral margins of stability, net mechanical work rate, and metabolic rate on step length asymmetry during early and late adaptation phases to determine if stability drives early adaptation and energetic cost drives late adaptation. Stability predicted SLA during the initial rapid onset of adaptation, and mechanical work rate predicted SLA during the latter part of adaptation. These findings suggest that stability optimization may contribute to early gait changes and that mechanical work contributes to later changes during adaptation. A final sub-analysis assessed the effect of aerobic capacity on step length asymmetry adaptation. Aerobic capacity levels below 36 and above 43 ml/kg/min resulted in greater adaptation, underscoring the metabolic influences on gait adaptation. This study illuminates the complex interplay between biomechanical and metabolic factors in gait adaptation, shedding light on fundamental mechanisms underlying human locomotion.

## Introduction

Adjusting gait to meet environmental demands is a critical and inherent feature of bipedal walking, thought to be accomplished through trial-and-error adaptation of typical walking patterns (Martin et al., 1996). In laboratory settings, gait adaptation can be assessed via split-belt treadmill walking, consisting of a treadmill with independently controlled belts moving at different speeds. Gait adaptation in response to treadmill walking is robust and observable through various kinematic and kinetic measures, including alterations in step lengths (Reisman et al., 2005; Sánchez et al., 2021), mediolateral margin of stability (Buurke et al., 2018), and mechanical work done by the legs (Sánchez et al., 2021, 2019; Selgrade et al., 2017). While these adaptive responses to split-belt perturbations have been consistently shown experimentally, the process(es) that drive these responses remain unknown.

Prior work has postulated that gait adaptation during split-belt treadmill walking is driven by error-based learning, where interlimb kinematic asymmetry serves as an error signal that the nervous system attempts to minimize over the course of adaptation (Malone et al., 2012; Reisman et al., 2005). While interlimb asymmetry does adapt, recent work has proposed a use-dependent learning framework (Wood et al., 2021) and has demonstrated that, with sufficient time and practice under novel walking conditions, people tend to adopt asymmetric gait patterns (Sánchez et al., 2021; Stenum and Choi, 2020) that reduce the energetic costs of walking (Finley et al., 2013; Sánchez et al., 2021, 2019). Additionally, the acquisition of a novel gait pattern can be influenced by reinforcement learning, where specific and binary kinematic feedback can drive the learning process (Wood et al., 2024). Recent simulation studies have demonstrated that gait adaptation in response to a continuous perturbation is driven first by modifying stability (Seethapathi et al., 2021, pre-print) and then by reducing metabolic cost (Price et al., 2023; Seethapathi et al., 2021). The hypothesis that early adaptation functions to maintain stability is supported by recent data demonstrating reduced early gait perturbation (i.e., within the first five strides) when participants are allowed to hold on to handrails (Park and Finley, 2022). This early phase of gait adaptation seems to correspond to the first of two timescales of adaptation in step length asymmetry (SLA) during continuous gait adaptation (Darmohray et al., 2019; Mawase et al., 2013; Roemmich et al., 2016; Sánchez et al., 2021). The second timescale may correspond to metabolic cost adaptation (Price et al., 2023; Seethapathi et al., 2021) and is supported by work suggesting that gait adaptation typically leads to asymmetric gait patterns if they result in reduced energetic cost (Sánchez et al., 2021; Stenum and Choi, 2020). The stability and energetic aspects of adaptation can be measured experimentally using mediolateral margin of stability (ML MoS) as a proxy for mediolateral stability (Buurke et al., 2018), using metabolic rate from indirect calorimetry as a proxy for metabolic cost (Buurke et al., 2018; Finley et al., 2013; Roemmich et al., 2019; Roper et al., 2013; Sánchez et al., 2021, 2019), and mechanical work by the legs as a proxy for mechanical cost (Buurke et al., 2018; Finley et al., 2013; Sánchez et al., 2021, 2019; Selgrade et al., 2017). Thus, we can objectively assess the underlying processes proposed to drive locomotor adaptation (Price et al., 2023; Seethapathi et al., 2021).

While our group and others have independently investigated kinematics, stability, metabolic rate, and mechanical work by the legs during gait adaptation (Brinkerhoff et al., 2023, 2021; Buurke et al., 2018; Darter, 2018; Finley et al., 2013; Park and Finley, 2022; Roemmich et al., 2019; Roper et al., 2019, 2017, 2013; Sánchez et al., 2021, 2019), the field has yet to explore the timescales of each of these processes and the relations between them. Thus, the primary purpose of this study was to comprehensively investigate the dynamics of gait adaptation by examining the interplay between stability, metabolic cost, and mechanical cost. Specifically, we aimed to unravel the intricate relations and timescales associated with kinematic measures of adaptation – SLA, fast-leg step length, slow-leg step length; measures of stability – ML MoS of the fast leg and ML MoS of the slow leg; and energetic measures, such as metabolic rate; and work done by the legs – net mechanical work rate, positive fast-leg mechanical work rate, negative fast-leg mechanical work rate, positive slow-leg mechanical work rate, and negative slow-leg mechanical work rate. We hypothesized two distinct timescales of adaptation; ML MoS, as a proxy for stability, would adapt quickly (Park and Finley, 2022; Seethapathi et al., 2021), while mechanical and metabolic work rates would adapt slowly (Darmohray et al., 2019; Mawase et al., 2013; Roemmich et al., 2016; Sánchez et al., 2021; Seethapathi et al., 2021). We also sought to define the relations between adaptation and the processes of adaptation (ML MoS, metabolic rate, and net mechanical work rate done by the legs). We hypothesized that ML MoS would predict initial but not later SLA, while mechanical work rate and metabolic cost would predict later but not initial SLA. Finally, to describe the role of metabolic capacity on gait adaptation, we regressed the  $\text{VO}_2$  peak from a graded exercise test on SLA and metabolic rate adaptations. This work will help inform the field on the objectives that drive gait adaptation in younger adults, which can provide nuanced insight to inform biomechanical models of gait, guide clinical decision-making and gait rehabilitation strategies, and develop/refine assistive gait technologies.

## Methods

### Participants

To determine sample size, we simulated samples of sizes  $N = 6\text{--}30$  from known parameters (determined from pilot data) for SLA, metabolic rate, and  $\Delta$ ML MoS of the fast leg. We compared the model estimates from each simulated sample to the actual model parameters. We used reasonable heuristics to determine the minimum sample size that resulted in stable estimates. Specifically, we identified the sample size  $N$  at which the standard deviation of the differences between the simulated model growth estimates ( $r_f$  and  $r_s$  in eq. 3) and the true estimates, from samples of size  $N - 30$ , was less than or equal to half the standard deviation of the differences observed in the full sample size range before  $N$ . This approach allowed us to identify the point at which the variability in our growth estimates stabilized. The minimum sample sizes to achieve stable estimates were determined for SLA ( $N=17$ ), metabolic rate ( $N=14$ ), and  $\Delta$  ML MoS ( $N=16$ ) of the fast leg.

We recruited  $n=17$  participants ( $n=17$ ) from a convenience sample of young adults aged 19-35 for participation in this study (**Table 1**). Participants were excluded if they reported cardiovascular, pulmonary, renal, metabolic, vestibular, or neurologic disorders; any lower-extremity injuries or surgeries in the past 12 months; or a prior anterior cruciate ligament injury. Participants completed written informed consent via Qualtrics prior to visiting the laboratory for participation. The Auburn University Institutional Review Board approved all procedures.

### Experimental Protocol

Participants completed demographic intake questions and four surveys via Qualtrics before visiting the laboratory. Participants completed the Godin Leisure-Time Exercise Questionnaire (Godin and Shephard, 1985) to estimate their weekly exercise over the past three months. Participants were excluded if they performed more than 750 MET-minutes per week of moderate-vigorous exercise (equivalent to 150 minutes of moderate exercise per week) to avoid the confounding effect of exercise on adaptation (Brinkerhoff et al., 2023). Participants also completed the Claustrophobia Questionnaire (Radomsky et al., 2001). Participants were excluded if they reported a claustrophobia

score greater than 48 or a restriction subscore greater than 32 (Radomsky et al., 2001) to prevent adverse events due to wearing the metabolic face mask. To describe the sample, participants completed the Adverse Childhood Experiences questionnaire which is scored 0 (better) – 10 (worse) (Felitti et al., 1998), the Pittsburgh Sleep Quality Index which is scored 0 (better) – 21 (worse) (Buysse et al., 1989), and questions about socioeconomic status, race, ethnicity, sex assigned at birth, gender identity, and leg dominance (where the dominant leg is the leg that they indicate they would kick a ball with).

Participants visited the lab twice. During Visit 1, participants completed a treadmill graded exercise test to volitional exhaustion (BSU/Bruce Ramp protocol (Kaminsky and Whaley, 1998)). Maximal oxygen consumption (i.e.,  $\text{VO}_2$  peak) was measured using indirect calorimetry (Parvomedics TrueOne2400, Sandy, UT) and was used to characterize aerobic capacity for our sample. Criteria for attainment of  $\text{VO}_2$  peak included achieving at least two of the following: an RER greater than 1.1, an RPE greater than 17 (6 to 20 scale), a heart rate within 10 beats per minute of their age-predicted maximum, and a plateau in  $\text{O}_2$  with increasing exercise intensity (American College of Sports Medicine, 2019).

During Visit 2 (scheduled within three months of the graded exercise test), participants completed the gait adaptation protocol on an split-belt treadmill (SBT) (Prokop et al., 1995; Reisman et al., 2005). Metabolic rate was measured breath-by-breath with indirect calorimetry (Parvomedics TrueOne2400, Sandy, UT). Kinematic data were recorded from reflective markers placed bilaterally on the anterior superior iliac spine and the lateral malleoli of the ankles using a 17-camera motion capture system (VICON; Vicon Motion Systems Ltd, Oxford, United Kingdom).

The experimental protocol is shown in **Fig. 1**. Participants were instructed not to use the treadmill handrails for the duration of treadmill walking. First, participants stood for 4 minutes to obtain their standing metabolic rate. Then, they walked for 6 minutes at 1.0 m/s (baseline), followed by at least 4 minutes of standing or until the participant's metabolic rate returned to standing baseline levels. We measured each participants' average step lengths during the last 5 strides of baseline to determine which leg naturally took a longer step when treadmill walking, and which leg naturally took a

shorter step. Participants then walked for 20 minutes with the belt speeds split, such that the belt under the leg that took a shorter step during tied baseline walking moved at 1.5 m/s, and the belt under the leg that took a longer step during tied baseline walking moved at 0.5 m/s (“adaptation”). Following adaptation, participants stood for at least 4 minutes or until their metabolic rate returned to standing metabolic rate. Finally, they walked for 4 minutes with the belts tied at 1.0 m/s (“deadadaptation”).

## Data Analysis

Kinematic data were recorded at 100 Hz and were lowpass filtered with a 4<sup>th</sup>-order Butterworth filter with a cutoff frequency of 6 Hz. Ground reaction force data were obtained for each leg using an instrumented SBT, recorded at 1000 Hz from two separate force plates, and lowpass filtered with a 4<sup>th</sup>-order zero-phase Butterworth filter with a cutoff frequency of 20 Hz.

### *Step length and step length asymmetry*

Step length was calculated for each leg as the distance between the ankle markers along the anterior-posterior walking axis at the ipsilateral foot strike. SLA was calculated and normalized to stride length (eq. 1).

$$\text{Step Length Asymmetry} = \frac{\text{step length}_{\text{fast}} - \text{step length}_{\text{slow}}}{\text{step length}_{\text{fast}} + \text{step length}_{\text{slow}}} \quad 1$$

Step length<sub>fast</sub> is the step length when the leg on the fast belt strikes the belt, and Step length<sub>slow</sub> is the step length when the leg on the slow belt strikes the belt. A negative SLA indicates that the leg on the slow belt is taking a longer step than the leg on the fast belt, and an SLA of zero indicates that the legs are taking steps of equal length.

### *Mediolateral margin of stability*

We calculated ML MoS at every frame as the distance (cm) in the frontal plane between the extrapolated center of mass and the base of support, as calculated by Buurke and colleagues (Buurke et al., 2018; Hof et al., 2005). Methods in-brief are



provided. Data from the two force plates were combined to simulate a single plate for ground reaction force (GRF) and for ML center of pressure (CoP). ML CoP was calculated from forces and moments. ML CoM acceleration was calculated by dividing ML GRF by body mass and was twice-integrated to obtain a ML CoM relative position. Summing ML CoM relative position and ML CoP determined the ML CoM absolute position (Schepers et al., 2009). The velocity of this ML CoM absolute position was used to calculate extrapolated center of mass (xCoM) to find ML MoS (Hof et al., 2005). Fast-leg ML MoS was defined as the ML MoS at slow-leg foot-off, and slow-leg ML MoS was defined as the ML MoS at fast-leg foot-off. We chose to assess ML MoS at contralateral toe-off because this is the point in the gait cycle when the center of mass transitions from one limb to the other, which is suggested to have the highest metabolic demand and potentially the lowest stability (Kuo et al., 2005). An ML MoS of zero would indicate the xCoM was directly over the CoP, negative values would indicate that the xCoM was more lateral than the CoP and the person would have to take a corrective step; and a positive ML MoS would indicate that the xCoM was more medial than the CoP. During typical walking, ML MoS is most often positive, where the larger a positive-value, the further that the xCoM was from crossing over the CoP, and therefore connoted a more stable position (Hof et al., 2005).

### **Metabolic rate**

We calculated gross energy expenditure for every breath (J/min) (Garby and Astrup, 1987). Metabolic rate was calculated by dividing energy expenditure by 60 seconds (J/s, W). Net metabolic rate was calculated by subtracting standing baseline energy ( $W_{\text{net}}$ ). Relative net metabolic rate was calculated by dividing net metabolic rate by the participant's mass in kg ( $W_{\text{net}}/\text{kg}$ , eq. 2).

$$E_{\text{gross}} = (4.960 * RER + 16.040) * V_{O_2} \quad 2$$

On average across 20 minutes of SBT walking adaptation, participants were working at a relative effort of 34.4% (SD = 7.1%) of their  $VO_2$  peaks (**Table 1**).



### ***Mechanical work rates***

We calculated positive and negative mechanical work generated by the legs with a custom MATLAB program that used a point-mass model to estimate mechanical work generated by the legs on the treadmill and on the center of mass (Sánchez et al., 2021, 2019; Selgrade et al., 2017). Force data were partitioned by strides and the center of mass accelerations in each direction were time-integrated to obtain the center of mass velocity. The instantaneous power of each leg was obtained by summing the power generated by the leg on the body and the power generated by the leg on the treadmill; we added the dot product of the center of mass velocity and the ground reaction force (power generated by the leg on the body) to the dot product of the belt velocity and force applied to the belt, which is the inverse of the ground reaction force (power generated by the leg on the treadmill). Positive and negative work done by the leg was obtained by separately calculating the time integral of the positive and negative instantaneous power over the stride. Finally, work done by the leg was transformed into mechanical work rate by dividing the positive and negative work by the stride duration to account for changing stride duration during adaptation.

### **Statistical Analyses**

All statistical analyses were conducted in R (R Core Team, 2020). Data are reported as mean and standard error of the mean (SEM). Because metabolic data were obtained on a per-second basis, we also measured gait data by time rather than steps to allow comparison of timescales across the different variables. Mixed-effects nonlinear regression models were fit to each measure with the ‘nlme’ package (Pinheiro et al., 2020). All models were fitted with a maximum likelihood estimation, and all models contained a random effect such that the outcome measure’s estimated plateau was allowed to vary by participant.

We first determined the timescale (in seconds) of adaptation of each of the 11 measures: (1) SLA, (2) fast-leg step length, (3) slow-leg step length, (4) ML MoS of the fast leg, (5) ML MoS of the slow leg, (6) metabolic rate, (7) net mechanical work rate done by the legs, (8) positive fast-leg mechanical work rate, (9) negative fast-leg mechanical work rate, (10) positive slow-leg mechanical work rate, and (11) negative

slow-leg mechanical work rate. We removed the data from the initial transient increase in metabolic rate due to the onset of exercise, to only estimate the adaptation of metabolic rate after exercise onset.

We fit dual-rate exponential models to each measure (eq.3), estimating the adaptation of each measure over two distinct timescales. In the two-exponent models,  $c$  was the estimated plateau if seconds went to infinity;  $a_f$  was the initial value of the fast timescale of adaptation;  $r_f$  was the growth rate of the fast timescale of adaptation;  $a_s$  was the initial value of the slow timescale of adaptation;  $r_s$  was the growth rate of the slow timescale of adaptation. For each measure, we confirmed that a two-exponential model fit the data better than a one-exponential model using AIC.

$$Outcome = \left( c + a_f * e^{-\frac{sec}{r_f}} + a_s * e^{-\frac{sec}{r_s}} \right) + (c|ID) \quad 3$$

We also binned each measure by “initial” and “later” adaptation phases. Initial adaptation included the biomechanic data from the start of adaptation until the time ( $r_f$ ) when the fast timescale of adaptation reached 63.2% of its final value, with metabolic data lagged 3 minutes behind to account for the time required for oxygen consumption and carbon dioxide production to reach a steady state (Sánchez et al., 2019; Selinger and Donelan, 2014). Later adaptation included biomechanic data from minutes 15 – 17 and metabolic data from minutes 18 – 20. Each measure was then averaged over three-second bins during each phase.

To test the hypothesis that stability drives initial stages of adaptation, and that energetic cost adaptation drives later stages of adaptation, linear mixed-effects models analyzed were used to analyze the interactions of epoch (initial SLA vs. later SLA adaptation) with fast- and slow-leg ML MoS and net mechanical work on SLA. A mixed-effects model also analyzed the interaction of epoch and SLA on the metabolic rate, which was lagged behind SLA by 3 minutes.

Finally, as a sub-analysis to follow up on a prior study (Brinkerhoff et al., 2023), we analyzed the relations between aerobic capacity and gait adaptation. To this end, the changes in SLA and metabolic rate at the end of adaptation were calculated. SLA and metabolic rate were each averaged over initial adaptation (0 to  $r_f$  seconds) and the

last 2 minutes of adaptation, and then initial adaptation values were subtracted from late adaptation values. Linear OLS regressions estimated the effect of gender-centered  $\text{VO}_2$  peak on SLA adaptation and on metabolic rate adaptation, covarying for gender (men, women) if gender significantly added to the model. Linear and quadratic relation models were compared.

## Results

SLA and step lengths changed as hypothesized; the fast leg took longer steps resulting in a more-positive SLA over 20 minutes of SBT walking (**Fig. 2**). SLA for all participants is shown in **Supplemental Fig. 1**. **Table 2** provides the means, standard errors of the mean (SEM), and significance levels for all adaptation coefficients. While we observed significant reductions in positive and negative work rates, primarily by the fast-leg (all timescales of adaptation  $p < 0.001$ , **Table 2**), in agreement with previous studies (Sánchez et al., 2021, 2019; Selgrade et al., 2017), here we will focus on the aggregate measure of net work rate. Below, we present a summary of the key results.

### *Margins of stability adapt quickly, while energetic costs adapt gradually*

The fast timescales of adaptation of SLA, fast-leg step length, and slow-leg step length were significant (SLA: Mean (M) = 23 sec, SEM = 2 sec,  $p < 0.001$ , **Fig. 3A**; fast-leg step length: M = 25 sec, SEM = 3 sec,  $p < 0.001$ , **Fig. 3B**; slow-leg step length: M = 4 sec, SEM = 1 sec,  $p = 0.006$ , **Fig. 3B**). Additionally, the slow timescales of adaptation of SLA, fast-leg step length, and slow-leg step length were also significant (SLA: M = 321 sec, SEM = 17 sec,  $p < 0.001$ , **Fig. 3A**; fast-leg step length: M = 210 sec, SEM = 9 sec,  $p < 0.001$ , **Fig. 3B**; slow-leg step length: M = 46 sec, SEM = 10 sec,  $p < 0.001$ , **Fig. 3B**).

ML MoS completed adaptation quickly, over a single, fast timescale (fast-leg: M = 40 sec, SEM = 5 sec,  $p < 0.001$ , **Fig. 3C**; slow-leg: M = 51 sec, SEM = 10 sec,  $p < 0.001$ , **Fig. 3C**). Conversely, both net metabolic rate (M = 353 sec, SEM = 37 sec,  $p < 0.001$ , **Fig. 3D**) and net mechanical work rate (M = 357 sec, SEM = 46 sec,  $p < 0.001$ , **Fig. 3E**) took longer to complete the slow timescale of adaptation).

***Stability predicts early SLA adaptation, while mechanical work predicts SLA adaptation over the entire trial***

Fast-leg ML MoS was found to depend on the epoch ( $F(1,1074.3)=33.028$ ,  $p<0.001$ ) such that during initial adaptation a larger fast-leg ML MoS predicted a more-positive SLA ( $p<0.001$ , **Fig. 4A**). Slow-leg ML MoS interacted with epoch ( $F(1,1069.4)=16.066$ ,  $p<0.001$ ) such that during initial adaptation, a smaller slow-leg ML MoS predicted a more-positive SLA was ( $p<0.001$  **Fig. 4B**). During later adaptation, there was no significant relation between ML MoS and SLA. Net mechanical work rate significantly predicted SLA during adaptation regardless of epoch such that a more-positive SLA was predicted by a more-negative net mechanical work rate ( $F(1,16.67)=13.599$ ,  $p=0.002$ , **Fig. 4C**). Net metabolic rate (lagged behind SLA by 3 minutes) did not predict SLA during either epoch (**Fig. 4D**).

***Individuals with either poor or excellent aerobic fitness adapt gait to a greater extent than those with average aerobic fitness***

The relations of  $VO_2$  peak with SLA and metabolic rate adaptation are shown in **Fig. 5**. The best-fitting model to predict changes in SLA was a quadratic model with no effect of gender (**Fig. 5A**). There was a significant convexity ( $B=0.001$ ,  $p=0.008$ ) and a significant negative tilt ( $B=-0.018$ ,  $p=0.015$ ). The model  $R^2$  was 0.41. Predicted SLA adaptation from the start to the end of 20 minutes was minimal (+0.04) at a  $VO_2$  peak of 39.4 ml/kg/min, and SLA adaptation increased as  $VO_2$  peak deviated in both directions. The best-fitting model to predict changes in metabolic rate was a linear model with no effect of gender (**Fig. 5B**). However, there was no evidence of a relation between  $VO_2$  peak and metabolic rate adaptation ( $p=0.873$ ), and the model  $R^2$  was 0.001.

## **Discussion**

This study determined the timescales of gait adaptation and mapped the relations between step adaptation and stability, metabolic cost, and mechanical cost adaptation. Stability adapted quickly and predicted SLA during the rapid initial phase of adaptation, emphasizing the role of stability in early gait adaptation. Conversely,

mechanical and metabolic rates adapted more gradually but only mechanical work rate predicted SLA during the later part of adaptation. Additionally, people with extreme aerobic fitness (high or low) adapted to a greater magnitude than those with average aerobic fitness. This study highlights the dynamic and shifting roles of stability and energetic cost during gait adaptation and presents novel findings on the influence of aerobic fitness on the extent of gait adaptation.

### ***Stability adapts rapidly and predicts early gait adaptation***

Mediolateral stability underwent rapid adaptation, contrasting with the slower adjustments observed in mechanical and metabolic rates. The rapid stability adjustment aligns closely with the initial adaptation of SLA and the step length of the fast leg, reinforcing the idea that stability adaptation may play a pivotal role in driving initial gait adjustments consistent with previous studies (Park and Finley, 2022; Seethapathi et al., 2021). Further, during initial adaptation, the ML MoS of both the fast and slow legs predicted subsequent SLA, indicating that stability adaptation influences the early but not later stages of gait adjustment. Interestingly, a more-positive SLA was associated with a larger fast-leg ML MoS but a smaller slow-leg ML MoS, suggesting that within the first ~30 seconds of adaptation, shifting the center of mass more over the slow leg contributes to a less-negative SLA. This CoM shift not only occurs in initial gait adaptation, but persists during later adaptation; ML MoS remains larger for the fast-leg and smaller for the slow-leg indicating that the CoM continues to stay more over the slow leg than the fast leg.

### ***Both metabolic and mechanical work adapt gradually, but only mechanical work predicts SLA during adaptation***

The dual rates of step length adaptation replicate prior work (Darmohray et al., 2019; Mawase et al., 2013; Roemmich et al., 2016; Sánchez et al., 2021). These results also support prior findings that SLA is increased and net mechanical work rate reduced primarily by lengthening the fast-leg step length, while the slow-leg step length does not change considerably (Sánchez et al., 2021). SLA, net mechanical work rate, and fast-leg mechanical work rates plateaued between 4 to 6 minutes, and metabolic rate

plateaued in 5.9 minutes. Prior work has shown that net mechanical work rate is directly related to metabolic rate (Burdett et al., 1983; Donelan et al., 2002; Sánchez et al., 2021, 2019; Wanta et al., 1993), and the current study suggests that metabolic rate lags behind gait mechanics by 1.5 to 2.5 minutes during 3:1 belt-speed ratio gait adaptation. The decreases in mechanical and metabolic rates are evidence that people make adjustments to reduce energy expenditure in a novel environment. However, while there was a strong relation between a more-negative net mechanical work rate and a more-positive SLA, there was no evidence of a relation between SLA and metabolic rate during initial nor later adaptation. Although unexpected, these results are not surprising; Buurke and colleagues similarly did not find a relation between the change in SLA and the change in metabolic power after 9 minutes of SBT walking (Buurke et al., 2018). Also, while both metabolic rate and mechanical work involve some measurement error, the assumptions made in estimating metabolic rate using indirect calorimetry are broader, making it less tightly linked to the specific biomechanical adaptations being measured. It is possible that longer periods of gait adaptation such as 45 minutes (Sánchez et al., 2021), and therefore larger amounts of data per participant, are necessary to observe the relation between metabolic power and adaptation.

It is important to note that the current study cannot dissociate stability from metabolic cost reduction. Mediolateral stability is a determinant of metabolic cost during typical walking and relates modestly to metabolic cost (Donelan et al., 2004, 2002). Stability optimization may contribute to reducing net mechanical work rate and metabolic rate, especially during initial adaptation. Future work should seek to determine the association between the rates of adaptation within individuals and the extent to which stability adaptation affects energetic adaptation.

***People at both ends of the aerobic fitness spectrum adapt to a greater extent than those with ‘average’ fitness***

A subanalysis uncovered an intriguing link between aerobic fitness and SLA adaptation. Our previous research noted slower and less extensive gait adaptation in individuals with higher habitual exercise levels than those with lower levels (Brinkerhoff et al., 2023). We hypothesized that the latter group’s greater adaptation might stem

from poorer aerobic fitness, but we lacked metabolic data to confirm this. Our current study provided a unique opportunity to explore the relation between magnitudes of adaptation and aerobic fitness. We found a convex relation between  $\text{VO}_2$  peak and SLA: individuals with aerobic fitness below 36 ml/kg/min and above 43 ml/kg/min adapted to a greater extent within 20 minutes than those with aerobic capacities between 36 and 43 ml/kg/min. Notably, the apex of this relation aligned with fitness categories of 'below average' for men (37–41 ml/kg/min) and 'average' for women (38–41 ml/kg/min) under the age of 25 (American College of Sports Medicine, 2019). However, our sample, limited to participants with less than 150 minutes per week of moderate-vigorous exercise, likely skewed towards lower aerobic fitness levels (Figure 5). We concede that it also may be that the two participants with  $> 45$  ml/kg/min  $\text{VO}_2$  peak are driving the J-curve. Future research should explore this relation in more aerobically heterogeneous samples, and in larger samples. These findings support the hypothesis that lower aerobic fitness drives adaptation to reduce relative energetic cost (Brinkerhoff et al., 2023); however, these findings also support the idea that higher aerobic fitness yields adeptness at reducing energetic cost, given that those who engage in more exercise can reach a minimum cost of transport during running while more sedentary adults do not (Cher et al., 2015). Individuals with below-average aerobic fitness adapt their gait to minimize energetic costs out of necessity, while those with above-average aerobic fitness do so out of capability.

Although our findings provide insight into how humans navigate novel environments, it is likely that some sensory feedback mechanisms influence the nervous system to produce the kinematic, kinetic, and metabolic outputs observed in this study. However, from the current data, we cannot infer causal relations between kinematics, kinetics, and metabolic cost, nor can we fully disentangle the factors driving stability from those reducing energetic cost. It has long been thought that mediolateral dynamic balance is internally measured by the relative location of the projected CoM (i.e., center of gravity) to the CoP (Winter, 1995). Additionally, recent work suggests that the nervous system does not rely on the feedback from global blood-gas receptors to optimize energetic cost during walking (Wong et al., 2017). Instead, it might use local proprioceptive signals from Golgi tendon organs and spindles to estimate the demand from individual



muscles and motor units, and to sense and adjust for specific muscle effort and potential fatigue, rather than for total-body energetic cost (Wong et al., 2017).

This study has several limitations. First, the sample studied were young adults and did not exercise regularly. While a more homogenous group improves statistical power and reduces the need for covariates, it also reduces generalizability to other populations. Future work should seek to understand the timescales of adaptation and the relations between gait, stability, and energetic cost in other populations. Second, we used a dual-rate model to measure gait adaptation. The results of this study and others (Brinkerhoff et al., 2023; Sánchez et al., 2021) suggest that a dual-rate model accurately represents multiple gait adaptation measures. While our analysis focused on the dual-rate theory, future research should explore alternative models as new theoretical frameworks emerge.

Gait adaptation is a complex and multifaceted task consisting of multiple simultaneous processes. Stability adjusts rapidly during the initial phase of adaptation, while energetic costs, reflected in metabolic and mechanical rates, adapt gradually over time. Notably, stability predicts early gait adjustments, suggesting its pivotal role in driving initial changes. Our findings highlight a complex interplay between biomechanical and metabolic factors, with metabolic rate lagging behind gait mechanics during adaptation. Surprisingly, while there is a strong association between net mechanical work rate and step length asymmetry, no such relation exists between metabolic rate and step length asymmetry. Our investigation also reveals a significant link between aerobic fitness and gait adaptation, with individuals at both ends of the fitness spectrum demonstrating greater adaptation than those with average fitness levels. These findings underscore the critical influence of biomechanical and metabolic factors in shaping gait adaptation strategies.

### **Competing interests**

No competing interests declared.

## Data availability

Data will be made publicly available on GitHub at time of publication.

## Diversity and inclusion statement

This work aimed to recruit and describe gait adaptation in a diverse sample of participants in regard to race, ethnicity, gender, sexuality, and socioeconomic status.

## References

- American College of Sports Medicine, 2019. ACSM's Guidelines for Exercise Testing and Prescription, Tenth. ed. Lippincott Williams & Wilkins.
- Brinkerhoff, S.A., Monaghan, P.G., Roper, J.A., 2021. Adapting gait with asymmetric visual feedback affects deadaptation but not adaptation in healthy young adults. *PLOS ONE* 16, e0247706. <https://doi.org/10.1371/journal.pone.0247706>
- Brinkerhoff, S.A., Sánchez, N., Roper, J.A., 2023. Habitual exercise evokes fast and persistent adaptation during split-belt walking. *PLOS ONE* 18, e0286649. <https://doi.org/10.1371/journal.pone.0286649>
- Burdett, R.G., Skrinar, G.S., Simon, S.R., 1983. Comparison of mechanical work and metabolic energy consumption during normal gait. *J. Orthop. Res.* 1, 63–72. <https://doi.org/10.1002/jor.1100010109>
- Buurke, T.J.W., Lamothe, C.J.C., Vervoort, D., 2018. Adaptive control of dynamic balance in human gait on a split-belt treadmill. *J. Exp. Biol.* 10.
- Buyse, D.J., Reynolds, C.F., Monk, T.H., Berman, S.R., Kupfer, D.J., 1989. The Pittsburgh sleep quality index: A new instrument for psychiatric practice and research. *Psychiatry Res.* 28, 193–213. [https://doi.org/10.1016/0165-1781\(89\)90047-4](https://doi.org/10.1016/0165-1781(89)90047-4)
- Cher, P.H., Stewart, I.B., Worringham, C.J., 2015. Minimum Cost of Transport in Human Running Is Not Ubiquitous. *Med. Sci. Sports Exerc.* 47, 307–314. <https://doi.org/10.1249/MSS.0000000000000421>
- Darmohray, D.M., Jacobs, J.R., Marques, H.G., Carey, M.R., 2019. Spatial and Temporal Locomotor Learning in Mouse Cerebellum. *Neuron* 102, 217–231.e4. <https://doi.org/10.1016/j.neuron.2019.01.038>
- Darter, B.J., 2018. Dynamic stability during split-belt walking and the relationship with step length symmetry 6.
- Donelan, J.M., Kram, R., Kuo, A.D., 2002. Mechanical work for step-to-step transitions is a major determinant of the metabolic cost of human walking. *J. Exp. Biol.* 205, 3717–3727.

- Felitti, V.J., Anda, R.F., Nordenberg, D., Williamson, D.F., Spitz, A.M., Edwards, V., Koss, M.P., Marks, J.S., 1998. Relationship of Childhood Abuse and Household Dysfunction to Many of the Leading Causes of Death in Adults. *Am. J. Prev. Med.* 14, 245–258. [https://doi.org/10.1016/S0749-3797\(98\)00017-8](https://doi.org/10.1016/S0749-3797(98)00017-8)
- Finley, J.M., Bastian, A.J., Gottschall, J.S., 2013. Learning to be economical: the energy cost of walking tracks motor adaptation: Split-belt adaptation reduces metabolic power. *J. Physiol.* 591, 1081–1095. <https://doi.org/10.1113/jphysiol.2012.245506>
- Garby, L., Astrup, A., 1987. The relationship between the respiratory quotient and the energy equivalent of oxygen during simultaneous glucose and lipid oxidation and lipogenesis. *Acta Physiol. Scand.* 129.
- Godin, G., Shephard, R.J., 1985. A simple method to assess exercise behavior in the community. *Can. J. Appl. Sport Sci.* 10, 141–146.
- Hof, A.L., Gazendam, M.G.J., Sinke, W.E., 2005. The condition for dynamic stability. *J. Biomech.* 38, 1–8. <https://doi.org/10.1016/j.jbiomech.2004.03.025>
- Kaminsky, L.A., Whaley, M.H., 1998. Evaluation of a New Standardized Ramp Protocol: The BSU/Bruce Ramp Protocol. *J. Cardpulm. Rehabil.* 18, 438–444.
- Kuo, A.D., Donelan, J.M., Ruina, A., 2005. Energetic Consequences of Walking Like an Inverted Pendulum: Step-to-Step Transitions: *Exerc. Sport Sci. Rev.* 33, 88–97. <https://doi.org/10.1097/00003677-200504000-00006>
- Malone, L.A., Bastian, A.J., Torres-Oviedo, G., 2012. How does the motor system correct for errors in time and space during locomotor adaptation? *J. Neurophysiol.* 108, 672–683. <https://doi.org/10.1152/jn.00391.2011>
- Martin, T.A., Keating, J.G., Goodkin, H.P., Bastian, A.J., Thach, W.T., 1996. Throwing while looking through prisms: I. Focal olivocerebellar lesions impair adaptation. *Brain* 119, 1183–1198. <https://doi.org/10.1093/brain/119.4.1183>
- Mawase, F., Haizler, T., Bar-Haim, S., Karniel, A., 2013. Kinetic adaptation during locomotion on a split-belt treadmill. *J. Neurophysiol.* 109, 2216–2227. <https://doi.org/10.1152/jn.00938.2012>
- Park, S., Finley, J.M., 2022. Manual stabilization reveals a transient role for balance control during locomotor adaptation. *J. Neurophysiol.* 128, 808–818. <https://doi.org/10.1152/jn.00377.2021>
- Pinheiro, J., Bates, D., DebRoy, S., Sarkar, D., R Core Team, 2020. nlme: Linear and Nonlinear Mixed Effects Models.
- Price, M., Huber, M.E., Hoogkamer, W., 2023. Minimum effort simulations of split-belt treadmill walking exploit asymmetry to reduce metabolic energy expenditure. *J. Neurophysiol.* 129, 900–913. <https://doi.org/10.1152/jn.00343.2022>
- Prokop, T., Berger, W., Zijlstra, W., Dietz, V., 1995. Adaptational and learning processes during human split-belt locomotion: interaction between central mechanisms and afferent input. *Exp. Brain Res.* 106. <https://doi.org/10.1007/BF00231067>
- Radomsky, A.S., Rachman, S., Thordarson, D.S., McIsaac, H.K., Teachman, B.A., 2001. The Claustrophobia Questionnaire. *J. Anxiety Disord.* 15, 287–297. [https://doi.org/10.1016/S0887-6185\(01\)00064-0](https://doi.org/10.1016/S0887-6185(01)00064-0)

- Reisman, D.S., Block, H.J., Bastian, A.J., 2005. Interlimb Coordination During Locomotion: What Can be Adapted and Stored? *J. Neurophysiol.* 94, 2403–2415. <https://doi.org/10.1152/jn.00089.2005>
- Roemmich, R.T., Leech, K.A., Gonzalez, A.J., Bastian, A.J., 2019. Trading Symmetry for Energy Cost During Walking in Healthy Adults and Persons Poststroke. *Neurorehabil. Neural Repair* 33, 602–613. <https://doi.org/10.1177/1545968319855028>
- Roemmich, R.T., Long, A.W., Bastian, A.J., 2016. Seeing the Errors You Feel Enhances Locomotor Performance but Not Learning. *Curr. Biol.* 26, 2707–2716. <https://doi.org/10.1016/j.cub.2016.08.012>
- Roper, J.A., Brinkerhoff, S.A., Harrison, B.R., Schmitt, A.C., Roemmich, R.T., Hass, C.J., 2019. Persons with essential tremor can adapt to new walking patterns. *J. Neurophysiol.* 122, 1598–1605. <https://doi.org/10.1152/jn.00320.2019>
- Roper, J.A., Roemmich, R.T., Tillman, M.D., Terza, M.J., Hass, C.J., 2017. Split-Belt Treadmill Walking Alters Lower Extremity Frontal Plane Mechanics. *J. Appl. Biomech.* 33, 256–260. <https://doi.org/10.1123/jab.2016-0059>
- Roper, J.A., Stegemöller, E.L., Tillman, M.D., Hass, C.J., 2013. Oxygen consumption, oxygen cost, heart rate, and perceived effort during split-belt treadmill walking in young healthy adults. *Eur. J. Appl. Physiol.* 113, 729–734. <https://doi.org/10.1007/s00421-012-2477-7>
- Sánchez, N., Simha, S.N., Donelan, J.M., Finley, J.M., 2021. Using asymmetry to your advantage: learning to acquire and accept external assistance during prolonged split-belt walking. *J. Neurophysiol.* 125, 344–357. <https://doi.org/10.1152/jn.00416.2020>
- Sánchez, N., Simha, S.N., Donelan, J.M., Finley, J.M., 2019. Taking advantage of external mechanical work to reduce metabolic cost: the mechanics and energetics of split-belt treadmill walking. *J. Physiol.* 597, 4053–4068. <https://doi.org/10.1113/JP277725>
- Schepers, H.M., Van Asseldonk, E., Buurke, J.H., Veltink, P.H., 2009. Ambulatory Estimation of Center of Mass Displacement During Walking. *IEEE Trans. Biomed. Eng.* 56, 1189–1195. <https://doi.org/10.1109/TBME.2008.2011059>
- Seethapathi, N., Clark, B., Srinivasan, M., 2021. Exploration-based learning of a step to step controller predicts locomotor adaptation (preprint). *Neuroscience*. <https://doi.org/10.1101/2021.03.18.435986>
- Selgrade, B.P., Thajchayapong, M., Lee, G.E., Toney, M.E., Chang, Y.-H., 2017. Changes in mechanical work during neural adaptation to asymmetric locomotion. *J. Exp. Biol.* jeb.149450. <https://doi.org/10.1242/jeb.149450>
- Selinger, J.C., Donelan, J.M., 2014. Estimating instantaneous energetic cost during non-steady-state gait. *J. Appl. Physiol.* 117, 1406–1415. <https://doi.org/10.1152/jappphysiol.00445.2014>
- Stenum, J., Choi, J.T., 2020. Step time asymmetry but not step length asymmetry is adapted to optimize energy cost of split-belt treadmill walking. *J. Physiol.* 598, 4063–4078. <https://doi.org/10.1113/JP279195>
- Wanta, D.M., Nagle, F.J., Webb, P., 1993. Metabolic response to graded downhill walking. *Med. Sci. Sports Exerc.* 25, 159–162.
- Winter, D., 1995. Human balance and posture control during standing and walking. *Gait Posture* 3, 193–214. [https://doi.org/10.1016/0966-6362\(96\)82849-9](https://doi.org/10.1016/0966-6362(96)82849-9)

- Wong, J.D., O'Connor, S.M., Selinger, J.C., Donelan, J.M., 2017. Contribution of blood oxygen and carbon dioxide sensing to the energetic optimization of human walking. *J. Neurophysiol.* 118, 1425–1433. <https://doi.org/10.1152/jn.00195.2017>
- Wood, J.M., Kim, H.E., Morton, S.M., 2024. Reinforcement Learning during Locomotion. *eneuro* 11, ENEURO.0383-23.2024. <https://doi.org/10.1523/ENEURO.0383-23.2024>
- Wood, J.M., Morton, S.M., Kim, H.E., 2021. The Consistency of Prior Movements Shapes Locomotor Use-Dependent Learning. *eneuro* 8, ENEURO.0265-20.2021. <https://doi.org/10.1523/ENEURO.0265-20.2021>

## Figures and Tables

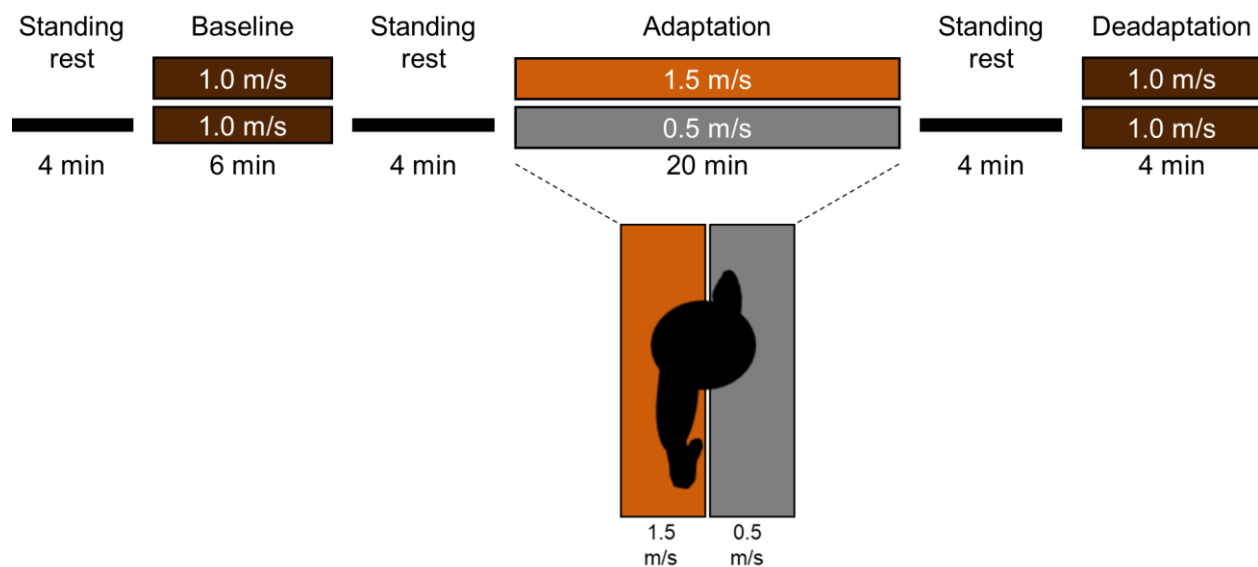


**Fig. 1. Experimental protocol.** Orange = fast-leg, grey = slow-leg. Participants stood for 4 minutes, followed by a 6-minute walk at 1.0 m/s (baseline). We measured each participant's average step lengths during the last 5 strides of baseline to determine which leg naturally took a longer step when treadmill walking, and which leg naturally took a shorter step. After a 4-minute break, participants walked for 20 minutes with the belt under the shorter-stepping leg moving at 1.5 m/s, and the belt under the longer-stepping leg moving at 0.5 m/s (adaptation). After another 4-minute break, participants walked for 4 minutes with the belts tied at 1.0 m/s (deadadaptation).

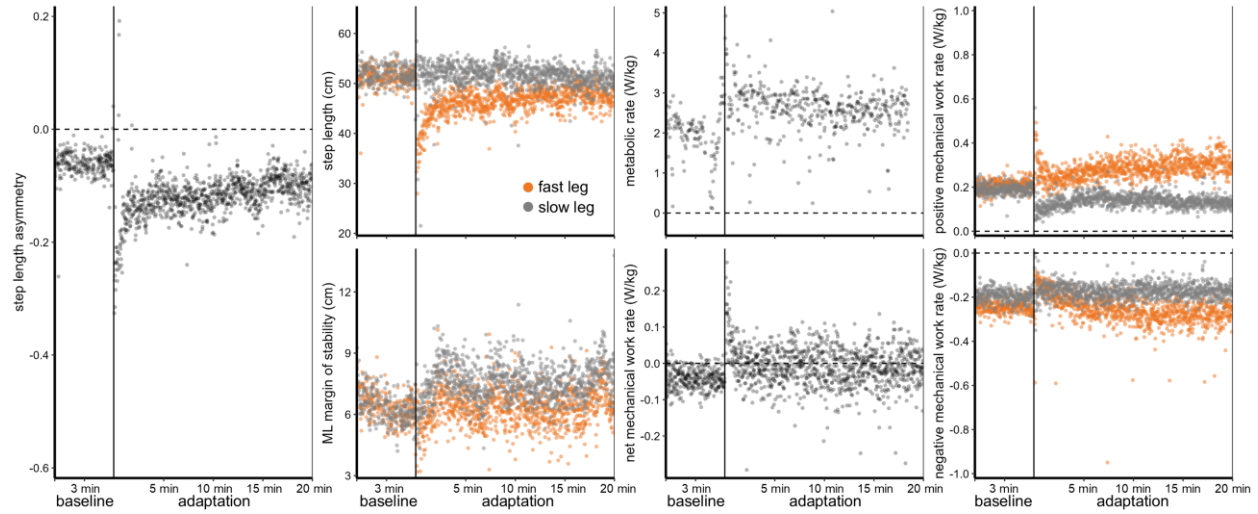


**Fig. 2.** Representative data from a single participant during baseline and adaptation for: step length asymmetry, step lengths, ML MoS, metabolic rate, and mechanical work rates.



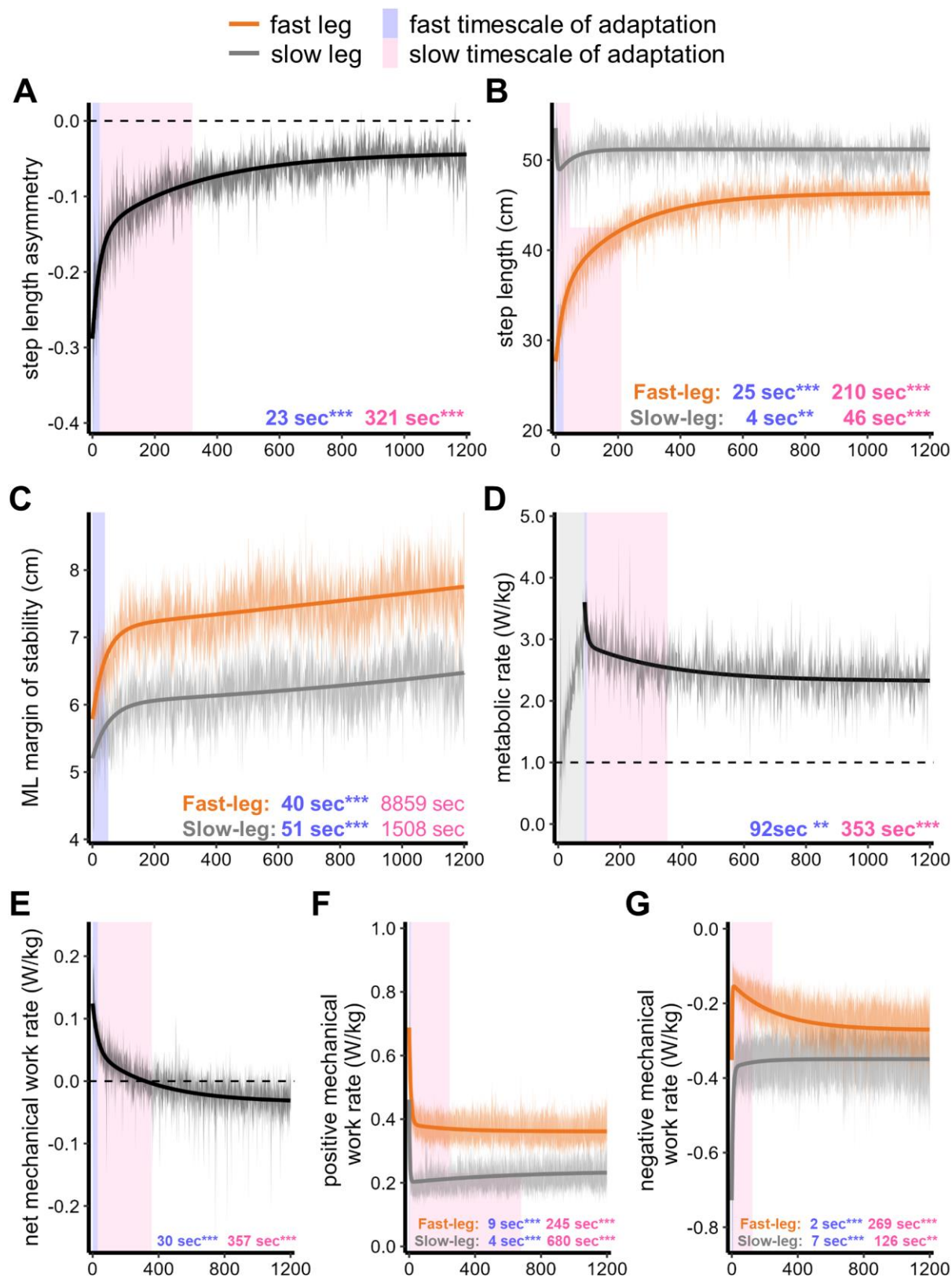


**Fig. 3. Dual-rate models of gait adaptation.** Lines indicate the model-estimated adaptation and shaded ribbons indicate standard error of the actual data. Orange = fast leg, grey = slow leg. The numbers and shaded plot areas indicate the rates of adaptation of the fast timescale (blue) and the slow timescale (pink). A) SLA, B) Step lengths, C) ML MoS, D) metabolic rate, where the vertical grey shaded rectangle indicates the metabolic rate that has been removed from analyses, E) net mechanical work rate, F) positive mechanical work rate, G) negative mechanical work rate. \*\*\* $p < 0.001$ , \*\* $p < 0.01$ .

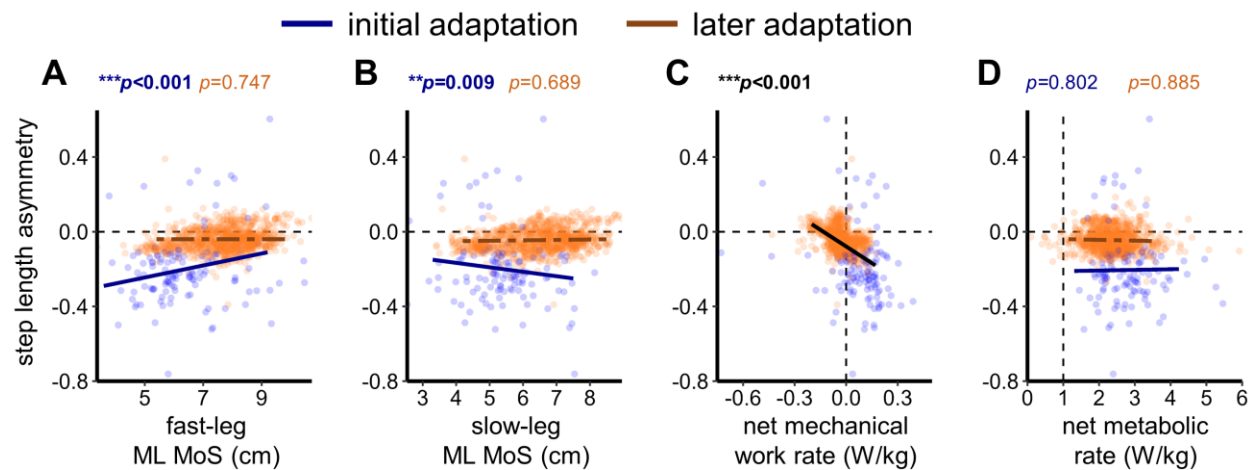


**Fig. 4. Linear mixed regressions predicting SLA during initial and later SLA adaptation.** Each data point represents the average over a binned 5-second interval for a participant, and all participants' data are shown. A-B) SLA was predicted by both fast-leg and slow-leg ML MoS during initial but not later adaptation. Blue points, solid lines, and p-values indicate the relation between SLA and ML MoS during initial SLA adaptation, and orange points, dashed lines, and p-values indicate the relation between SLA and ML MoS during later SLA adaptation. C). SLA was predicted by net mechanical work rate during the entirety of gait adaptation, regardless of adaptation phase. Blue points indicate initial adaptation, orange points indicate later adaptation, and the black line and p-value indicate the relation between SLA and net mechanical work rate during the entirety of SLA adaptation. D) SLA was not predicted by net metabolic rate during gait adaptation. Blue points, solid line, and p-values indicate the relation between SLA and net metabolic rate during initial SLA adaptation, and orange points, dashed line, and p-values indicate the relation between SLA and net metabolic rate during later SLA adaptation.

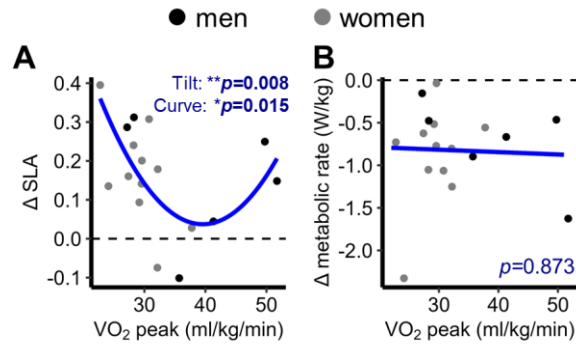


**Fig. 5. The relations between  $VO_2$  peak and adaptation of A) SLA and B) net metabolic rate.** Points reflect the change from the first 23 seconds of adaptation to the final 2 minutes of adaptation. Men are represented by black points, and women are represented by gray points, though gender did not affect the relations between outcomes and  $VO_2$  peak. Lines indicate the model-estimated relation.

**Table 1. Sample characteristics.**

Characteristic	<i>n</i>	Mean (SD)	Characteristic	<i>n</i>
Age	17	22 (3)	<i>Gender</i>	
Mass (kg)	17	73.5 (15.0)	Cisgender	17
Height (cm)	17	171.8 (7.6)	Trans gender binary	0
Leg length (m)	17	0.79 (0.05)	Trans gender non-binary	0
Days between visits	17	13 (10)	<i>Race</i>	
CQ total	17	22 (11)	White	16
CQ restriction subscore	17	14 (7)	Black or African American	0
MVPA MET-min per week	17	320 (203)	American Indian or Alaskan Native	0
ACES	17	1 (2)	Asian	0
PSQI	17	5 (3)	Native Hawaiian or Pacific Islander	0
TST (hours)	17	7.5 (0.8)	Other race not listed	1
<i>VO<sub>2</sub> peak (ml/kg/min)</i>			<i>Ethnicity</i>	
Male	6	39.0 (10.5)	Hispanic/Latinx	3
Female	11	29.4 (4.1)	Not Hispanic/Latinx	14
<i>Average VO<sub>2</sub> during SBT walking (ml/kg/min)</i>			<i>Approximate household income</i>	

	Male	6	11.1 (1.4)	< \$12,760	4
	Female	11	10.7 (1.0)	\$12,761 — \$24,999	2
<i>Relative Effort during SBT walking (% VO<sub>2</sub> peak)</i>				\$25,000 — \$49,000	2
	Male	6	29.6 (5.9)	\$50,000 — \$74,999	1
	Female	11	37.0 (6.6)	\$75,000 — \$99,999	2
<i>Dominant leg</i>				\$100,000 — \$124,999	3
	Left	1		\$125,000 — \$149,999	0
	Right	16		>=150,000	2
<i>Leg on the fast belt</i>					
	Dominant	8			
	Nondominant	9			

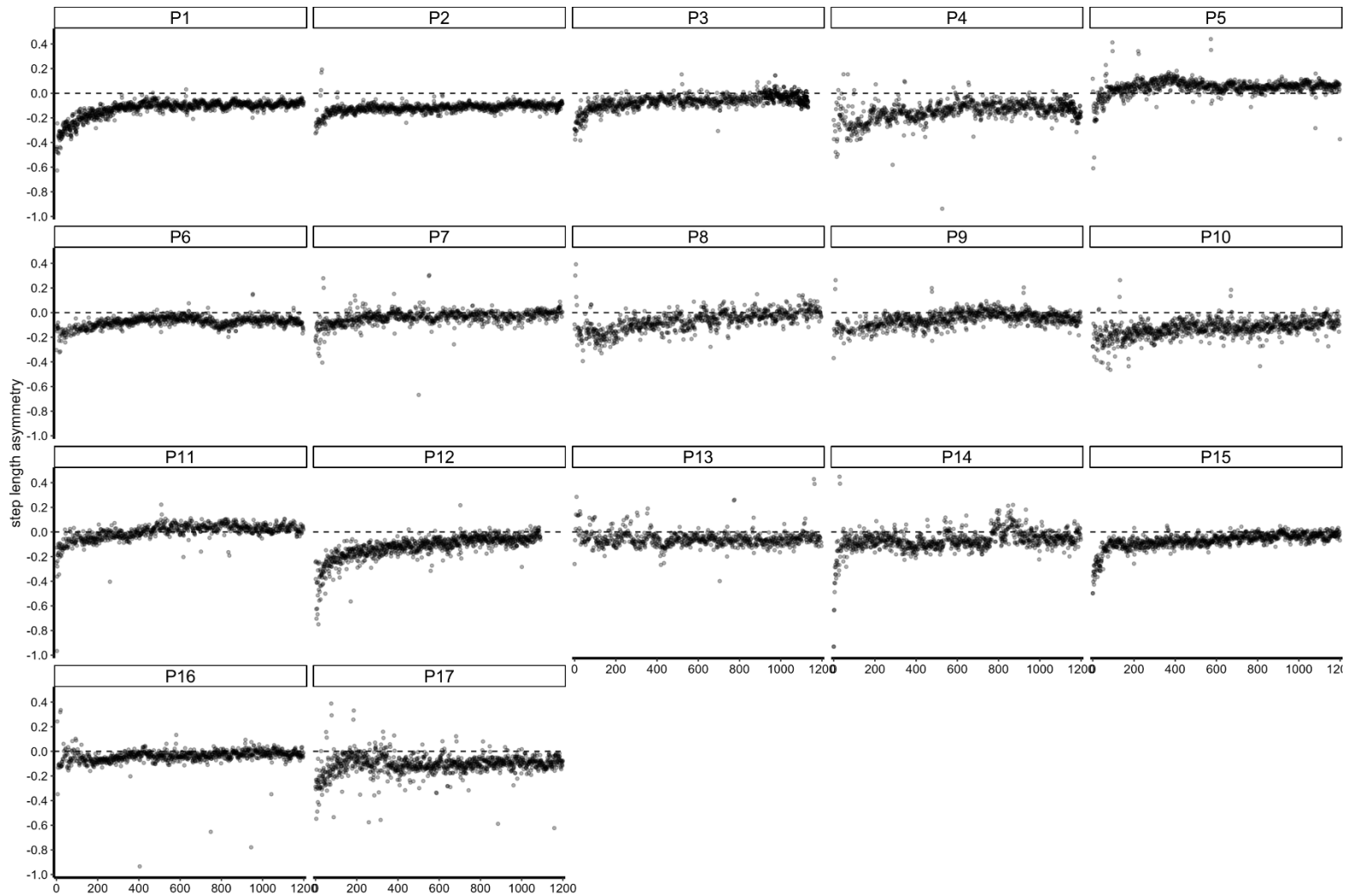
*CQ = Claustrophobia Questionnaire; MVPA = moderate to vigorous physical activity; ACES = Adverse Childhood Events Survey; PSQI = Pittsburgh Sleep Questionnaire Index; TST = total sleep time (from the PSQI). Leg dominance was only used to characterize the sample in this study, where the dominant leg was the leg participants indicated they would kick a ball with.*

Table 2. Nonlinear Mixed Model Estimates of the Timescales of Adaptation

		Fast				Net		Slow			
		Fast	Slow			Metaboli	mechanic	Fast	Fast	Slow	negative
	SLA	step	step	Fast	Slow	c	al	positive	negative	positive	work
		length	length	MOS	MOS	rate	work rate	work rate	work rate	work rate	rate
$c$	<b>-0.04***</b>	<b>46.34***</b>	<b>51.19***</b>	2.99	<b>5.65***</b>	<b>2.32***</b>	<b>-0.03**</b>	<b>0.36***</b>	<b>-0.27***</b>	<b>0.24***</b>	<b>-0.35***</b>
	(0.01)	(0.96)	(0.80)	(17.69)	(0.56)	(0.07)	(0.01)	(0.04)	(0.05)	(0.04)	(0.06)
$a_f$	<b>-0.14***</b>	<b>-7.59***</b>	<b>5.52***</b>	<b>-1.36***</b>	<b>-0.82***</b>	<b>0.69***</b>	<b>0.08***</b>	<b>0.30***</b>	<b>-0.20***</b>	<b>0.26***</b>	<b>-0.35***</b>
	(0.01)	(0.47)	(0.98)	(0.09)	(0.07)	(0.13)	(0.01)	(0.01)	(0.02)	(0.01)	(0.01)
$r_f$	<b>22.90***</b>	<b>24.60***</b>	<b>3.65**</b>	<b>40.27***</b>	<b>50.95***</b>	<b>92.19**</b>	<b>30.24***</b>	<b>9.30***</b>	<b>2.33***</b>	<b>3.91***</b>	<b>6.69***</b>
	(1.87)	(3.02)	(1.33)	(5.26)	(9.59)	(2.71)	(6.36)	(0.60)	(0.40)	(0.30)	(0.50)
$a_s$	<b>-0.11***</b>	<b>-11.11***</b>	<b>-3.15***</b>	4.16	0.37	<b>0.60***</b>	<b>0.08***</b>	<b>0.02***</b>	<b>0.12***</b>	<b>-0.04***</b>	<b>-0.02***</b>
	(0.003)	(0.37)	(0.62)	(17.65)	(0.49)	(0.04)	(0.005)	(0.003)	(0.003)	(0.004)	(0.01)
$r_s$	<b>321.19***</b>	<b>209.85***</b>	<b>46.30***</b>	-8858.67 (34856.64)	-1508.13 (1342.64)	<b>352.92***</b>	<b>357.33***</b>	<b>245.08***</b>	<b>269.10***</b>	<b>680.09***</b>	<b>125.57**</b>
	(17.24)	(8.60)	(10.02)			(37.33)	(45.70)	(70.25)	(14.63)	(177.86)	(42.04)
Num. obs.	31929	16032	16029	15898	15904	8547	17531	17531	17531	17531	17531
Num. groups: id	17	17	17	17	17	17	17	17	17	17	17
$c$ (StDev)	0.049	3.952	3.288	0.607	0.662	0.281	0.053	0.165	0.206	0.163	0.254
Residual (StdDev)	0.068	3.608	4.184	1.0639	0.990	0.663	0.078	0.075	0.087	0.060	0.084



*Note. Model parameters are given as Coefficient (SEM), p-value. The best-fitting model to the data for all five outcome measures was the two-exponent model. All models contain a random plateau on participant. Asterisks indicate significant effects where \* $p < 0.05$ , \*\* $p < 0.01$ , \*\*\* $p < 0.001$ . The analysis was conducted on the metabolic rate data after the initial transient change in metabolic rate. The rate values in the table ( $r_f$  and  $r_s$ ) are the model values added to the mean time of the initial transient change in metabolic rate (84.8 seconds) so that the rate values are consistent with the start of the trial and the other outcome measures.*



**Fig. S1. Step length asymmetry over the entirety of 20 minutes of split-belt treadmill walking.** The representative participant in Figure 2 was *P15* and the two participants that did not achieve a positive change in step length asymmetry from initial to alter adaptation were *P13* and *P16*.